DOR: 20.1001.1.2322388.2020.8.3.2.5

Research Paper

Novel BCP-Bioactive Glass-Akermanite/PCL Composite Scaffold: Physical and Mechanical Behavior, and in Vitro Bioactivity

Ebrahim Karamian*, Shakiba Saghirzadeh darki

Advanced Materials Research Center, Department of Materials Engineering, Najafabad Branch, Islamic Azad University, Najafabad, Iran

ARTICLE INFO

Article history:

Received 8 August 2019
Accepted 8 March 2020
Available online 10 July 2020

Keywords:

Akermanite
Bioactive Glass
Bioactivity
Composite

ABSTRACT

In the present study, biphasic calcium phosphate (BCP)-bioactive glass-akermanite/PCL composite scaffold with high porosity (80%) was successfully fabricated using polymeric sponge replication and dip–coating methods. The composite was characterized via X-ray diffraction (XRD) and scanning electron microscopy (SEM). In addition, physical and mechanical properties of the composite were evaluated using porosity and compressive strength measurements. In vitro bioactivity of the composite was carried out using simulated body fluid solution (SBF). Results showed that PCL, as a polymeric coating, incremented the mechanical strength of ceramic scaffolds from 0.97 to 1.9MPa, confirming its fundamental role in recovering the mechanical properties of scaffolds in bone tissue engineering. Bioactivity evaluation resulted in developing an apatite–like layer on the surface of the scaffolds, which verified the proper bioactivity of the scaffolds. The results showed that this novel composite scaffold has the potential to be applied as a temporary substrate for bone tissue engineering.

* **Corresponding Author:**
E-mail Address: karamian1970@gmail.com

1. Introduction

Bone injury is considered one of the challenges of medical science which imposes a high cost to cure. Tissue engineering helps to restore injured tissues. Nowadays, tissue engineering is applied to restore and repair different tissues such as bone, cartilage, etc. [1, 2]. The main aim of tissue engineering is to fabricate scaffolds such as bony scaffolds with ideal mechanical and biological properties in order to restore injured tissues [3, 4]. Various methods such as electrospinning, freeze drying, solvent casting, polymeric sponge replication, etc. exist to fabricate the scaffolds. [5–8]. Fabricating the scaffolds with interconnected porous structures and proper toughness is considered a great challenge Since the scaffolds should possess appropriate chemical, physical, mechanical and biological properties so that they can be applied in bone tissue engineering [9, 10]. Bone consists of a porous composite with a combination of hydroxyapatite and collagen [11]. Therefore, fabricating a composite scaffold with properties such as bioactivity, physical and mechanical properties is important for bone tissue engineering applications [12].

Due to their bioactivity, bioceramics, such as hydroxyapatite, beta tricalcium phosphate, biphasic calcium phosphate (BCP), bioactive glass, akermanite ($Ca_2MgSi_2O_7$), etc. [13, 14] can be applied in fabricating the scaffolds. Among them, hydroxyapatite and beta tricalcium phosphate are similar to bone mineral component. On the other hand, bioactive glass can enhance the bioactivity of the scaffolds. Moreover, akermanite can enhance the mechanical properties of the scaffolds because of incorporating Mg^{2+} into Ca–Si network resulting in network stability. In addition, Si^{4+} in akermanite compound can improve the bioactivity behavior related to the scaffolds [15-18]. In contrast, due to their unique properties such as biocompatibility, high toughness and availability, biopolymers, further divided into natural and synthetic, play a significant role in fabricating scaffolds. One of the synthetic biopolymers is polycaprolactone (PCL), which is a semi-crystalline polymer with a melting point about 60℃. It possesses outstanding features such as biocompatibility, biodegradability, high toughness, availability and processability [19-21].

The aim of the present study is to fabricate and characterize a biphasic calcium phosphate(BCP)-based scaffold with calcium silicate and polymer reinforcing such as bioactive glass, akermanite and PCL in order to improve the mechanical and biological features of scaffolds for bone tissue engineering applications.

2. Materials and Methods

2.1. Raw materials

Raw materials for the synthetization of bioceramics include TEOS ($(C_2H_5O)_4$ Si) (Merck), magnesium nitrate ($Mg(NO_3)_2 . 6H_2O$) (Merck), calcium nitrate ($Ca(NO_3)_2 . 4H_2O$), distilled water (H_2O), nitric acid (HNO_3, 2M) (Merck), β – tricalcium phosphate ($Ca_3(PO_4)_2$), natural hydroxyapatite ($Ca_5(PO_4)_3(OH)_2$), silica powder (SiO_2) (Merck), phosphorous oxide powder (P_2O_5) (Merck), triethyl phosphate ($C_6H_{15}O_4P$) (Sigma Aldrich) and ethanol (C_2H_5OH) (Merck).

Raw materials for the fabrication of scaffolds include biphasic calcium phosphate (BCP), bioactive glass powder (63S), akermanite powder ($Ca_2MgSi_2O_7$), polymeric sponge, distilled water, carboxymethyl cellulose (CMC), sodium tripolyphosphate (STPP), chloroform (Merck) and polycaprolactone (PCL).

2.2. Synthesis of biphasic calcium phosphate powder (BCP)

Biphasic calcium phosphate powder was synthesized via ball milling method. Weight percentages of hydroxyapatite and β–tricalcium phosphate were considered 70 and 30, respectively, for ball milling; the time and speed of milling were 1 hour and 300 Rpm, respectively.

2.3. Synthesis of bioactive glass powder

In the present research, bioactive glass powder (63S) synthesized by sol–gel method according to previous researches [22] was utilized. The powder possessed SiO_2 (65%), P_2O_5 (31%) and CaO (4%). To synthesize the powder, TEOS (27ml), deionized water (9.6ml), and HCl (2N)(1.5ml) were added to ethanol (60ml). The solution was stirred with a speed of 1200rpm at ambient temperature for 30 minutes to obtain a homogenous solution. Afterwards, phosphate triethyl (2.3ml) was added to the solution, and it was stirred for 20 minutes. Finally, calcium nitrate (10.5g) was added to the solution, and it was stirred for 60 minutes. The obtained solution was put into oven at 60ºC for 48 hours. The obtained dried powder was calcinated at 600ºC with a rate of 5ºC/min for 2 hours.

2.4. Synthesis of akermanite powder

Akermanite bioceramic was synthesized via sol–gel method. In this method, TEOS, nitric acid and ethanol were dissolved for 30 minutes. Afterwards, calcium and magnesium nitrates were added to the solution, and the solution was stirred for 5 hours so that a homogenous solution was obtained. Subsequently, the obtained solution was dried at 60℃ and 100 ℃ for 1 and 2 days, respectively. Finally, the dried gel was calcinated at 1200℃ for 3 hours [23].

2.5. Fabrication of scaffolds

Polymeric sponge replication method was applied to fabricate bioceramic scaffolds. First, a ceramic slurry was prepared using double–distilled water, bioceramic powders such as BCP, bioactive glass and akermantie, carboxymethyl cellulose (CMC, 1.5wt%) and sodium tripolyphosphate (STTP, 2wt%). Afterwards, sponges were immersed into the ceramic slurry several times. Then, the sponges, impregnated with ceramic slurry, were dried at 80℃ for 12 hours. Subsequently, they were sintered at 1200℃ for 2 hours with a rate of 2℃/min so that porous bioceramic scaffolds were obtained. After that, PCL solution was prepared. Optimum bioceramic scaffold was coated using the PCL solution for 10 seconds. In the following, the scaffold was put into vacuum for 24 hours; and finally, the scaffold was dried in an oven at 40℃ for 24 hours.

2.6. Characterization of the scaffolds

2.6.1. Phase analysis (XRD)

XRD patterns were prepared from bioceramic powders and the scaffolds in order to investigate the developed phases related to the powders and scaffolds. The patterns were obtained using Philips device PW3040 model, CuK∝ tube with a wavelength of 1.54018 and diffracted angles of 10–90 degrees.

2.6.2. Fourier transform infrared spectroscopy (ATR – FTIR)

ATR–FTIR spectrum was prepared utilizing BRUKER device Tensor 27 model in the wavenumber range of 500–4000 cm^{-1} with a resolution of 4 cm^{-1} to examine the chemical bonds and functional groups in the scaffold.

2.6.3. Dynamic laser scattering (DLS)

DLS tests were prepared in order to examine particles size relevant to bioceramic powders.

2.6.4. Scanning electron microscopy (SEM)

The morphologies of the scaffolds were investigated via SEM images. Moreover, studies related to apatite–like layer were carried out by SEM images and EDS analysis. The images were provided via FEI, QUANTA 200 device.

2.6.5. Measurement of open porosity

Open porosity of the scaffolds was measured by liquid displacement method and equation 1 [24].

$$\text{Porosity } (\%) = \frac{V_1 - V_3}{V_2 - V_3} \times 100$$

Whereas V_1: Initial volume of ethanol

V_2: Ethanol volume related to immersion of the scaffolds

V_3: Remaining volume of ethanol

2.6.6. Mechanical strength

Measurement of mechanical strength (compressive strength) relevant to the scaffolds was carried out using Hounsfield device, H25KS model, and the applied force was 500N. Sizes of the scaffolds were considered 2 × 1 × 1 cm^3 according to ASTM–D5024–95a standard.

2.7. Bioactivity evaluation

Bioactivity of the scaffolds was evaluated using simulated body solution (SBF), prepared by Kokubo method [25]. The scaffolds were immersed in calibrated falcons containing SBF solution for 28 days.

It is noteworthy that the scaffolds were named in the present study as follows:

Scaffold B_0: BCP

Scaffold B_5: BCP + 5wt% of bioactive glass

Scaffold B_5A_2: BCP + 5wt% of bioactive glass + 2wt% of akermanite

Scaffold B_5A_5: BCP + 5wt% of bioactive glass + 5wt% of akermanite

Scaffold B_5A_2P: BCP + 5wt% bioactive glass + 2wt% akermanite + 6(w/v %) of PCL

3. Results and discussion

3.1. Characterization of bioceramic powders

3.1.1. Hydroxyapatite (HA)

Fig. 1(a) exhibits XRD pattern related to hydroxyapatite powder. It also verifies that all peaks matched with hydroxyapatite (HA) phase ($Ca_5(PO_4)_3(OH)$) (JCPDS 00-024-033). The issue proves the formation of hydroxyapatite.

Figure 2 exhibits the DLS test related to average particles size related to the hydroxyapatite powder. The result showed that the obtained average particles sizes was about 84.07 nm. In other words, the majority of particles were less than 100 nm. The issue verifies the formation of nano–hydroxyapatite powder, which is applied to synthesize biphasic calcium phosphate. It can be concluded that nano–hydroxyapatite plays a significant role in improving biphasic calcium phosphate properties such as mechanical and biological properties.

3.1.2. Beta tricalcium phosphate (β – TCP)

Fig. 1(b) exhibits the XRD pattern related to beta tricalcium phosphate powder. All peaks matched beta tricalcium phosphate phase (β – TCP) ($Ca_3(PO_4)_2$) (JCPDS 00-009-0169). The issue verifies perfect formation of beta tricalcium phosphate.

3.1.3. Bioactive glass

Fig. 1(c) exhibits the XRD pattern related to bioactive glass powder. It clearly verifies the amorphous peaks. The structure of bioactive glass is not crystalline. Therefore, it can be concluded that synthesis of bioactive glass was properly carried out via sol–gel method.

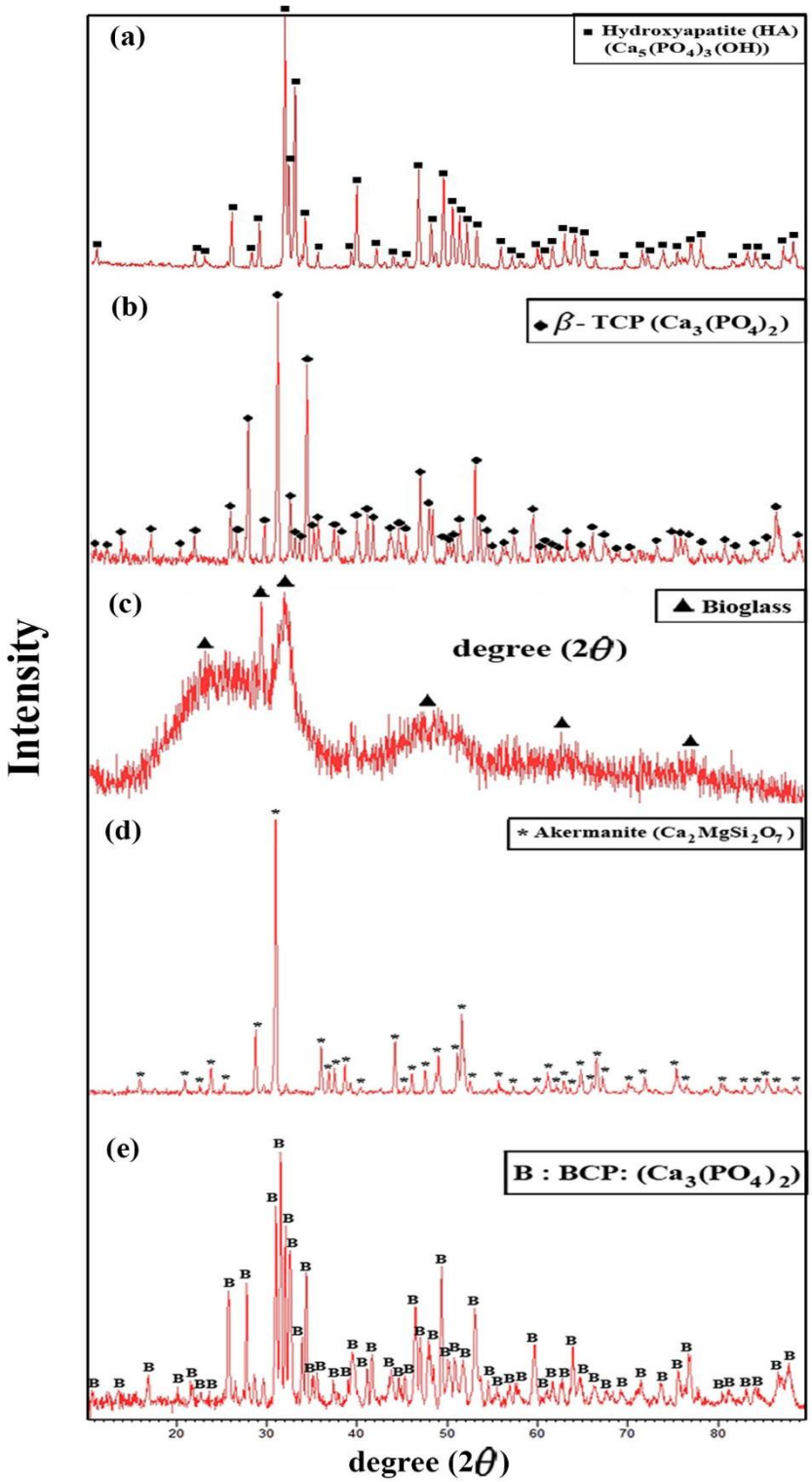

Fig. 1. XRD patterns :(a) hydroxyapatite, (b) tricalcium phosphate, (c) bioglass, (d) akermanite, and (e) biphasic calcium phosphate

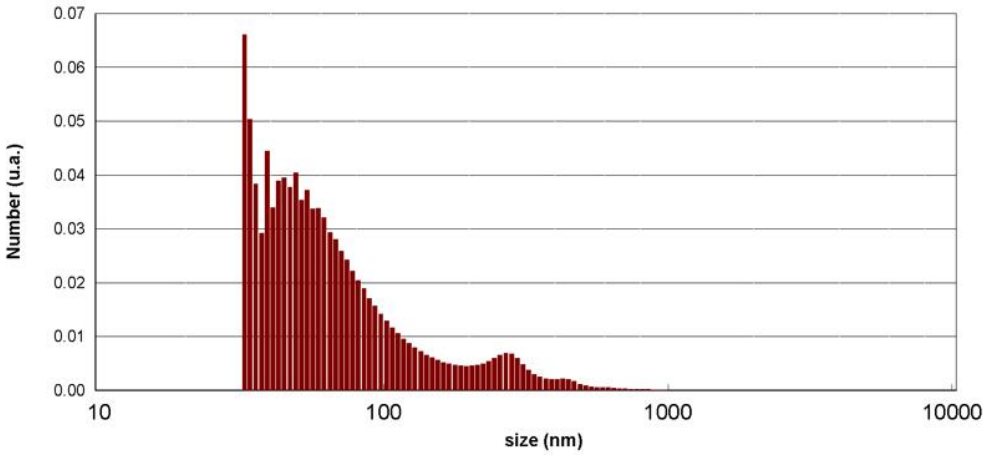

Fig. 2. DLS test related to hydroxyapatite powder

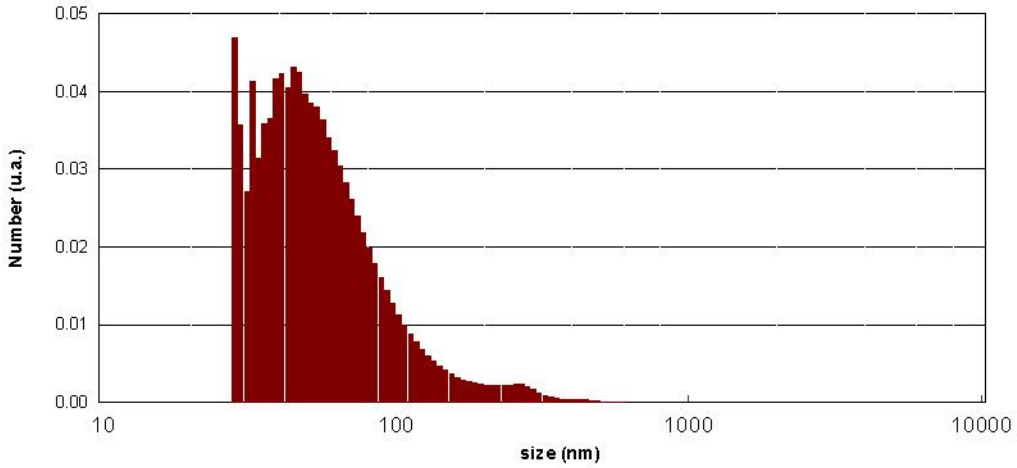

Fig.3. DLS test of bioactive glass

Fig. 3 exhibits the DLS test related to average particles size of bioactive glass powder, which was obtained about 62.76 nm. In other words, the majority of bioactive glass particles were less than 100 nm. In the present study, nano–bioactive glass was utilized as reinforcing in fabricating composite scaffolds. Nano–bioactive glass can affect the bioactivity of scaffolds.

3.1.4. Akermantie ($Ca_2MgSi_2O_7$)

Fig. 1(d) depicts the XRD pattern related to akermanite powder. The pattern confirms good correspondence of all peaks with akermanite ($Ca_2MgSi_2O_7$) (JCPDS 01-083-1815). It can be concluded that synthesis of the akermanite powder was conducted using sol–gel method properly.

Fig. 4 presents the DLS test related to average particles size of akermanite powder, which was obtained about 40.57 nm. The majority of the particles were less than 100 nm. Nano–akermanite was applied as reinforcing in fabricating composite scaffolds. Nano–akermanite plays a key role in improving mechanical properties such as compressive strength, and biological properties such as bioactivity of the scaffolds.

3.1.5. Biphasic calcium phosphate powder (BCP)

Fig. 1(e) exhibits the XRD pattern related to biphasic calcium phosphate powder. The pattern verifies the formation of biphasic calcium phosphate phase ($Ca_3(PO_4)_2$) (JCPDS 00-025-0167) with respect to all peaks. With regard to the pattern, the synthetization of the powder was carried out using ball milling clearly. It can be concluded that regarding the formation of biphasic calcium phosphate phase, the ideal selections were 1 hour to mill hydroxyapatite and beta calcium phosphate powders and, on the other hand, specific weight ratio of 70 to 30.

It can be discussed that all bioceramics possessed a single phase. The issue confirms phase decomposition in all bioceramic powders. Moreover, the majority of bioceramics possessed nanoparticles. Nano–bioceramics possess unique features such as high mechanical and great biological properties so that the development of an apatite–like layer was performed on their surface perfectly [26, 27].

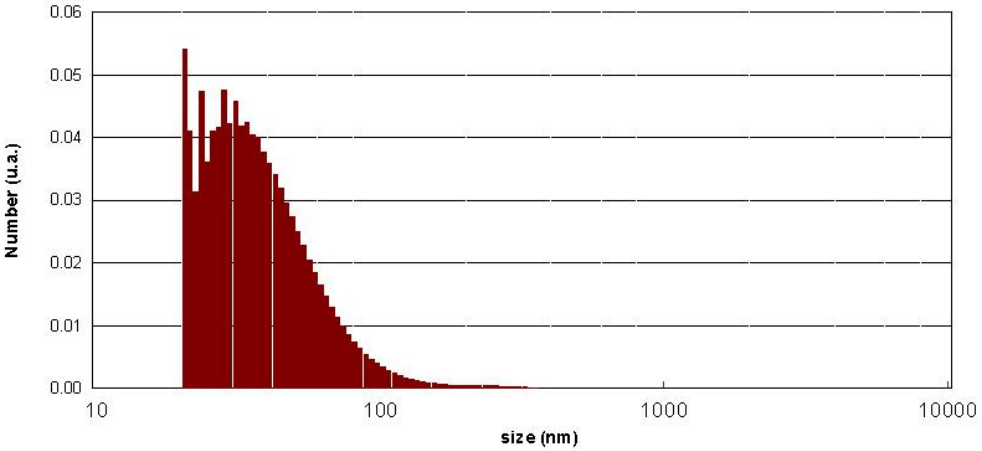

Fig. 4. DLS test relevant to akermanite

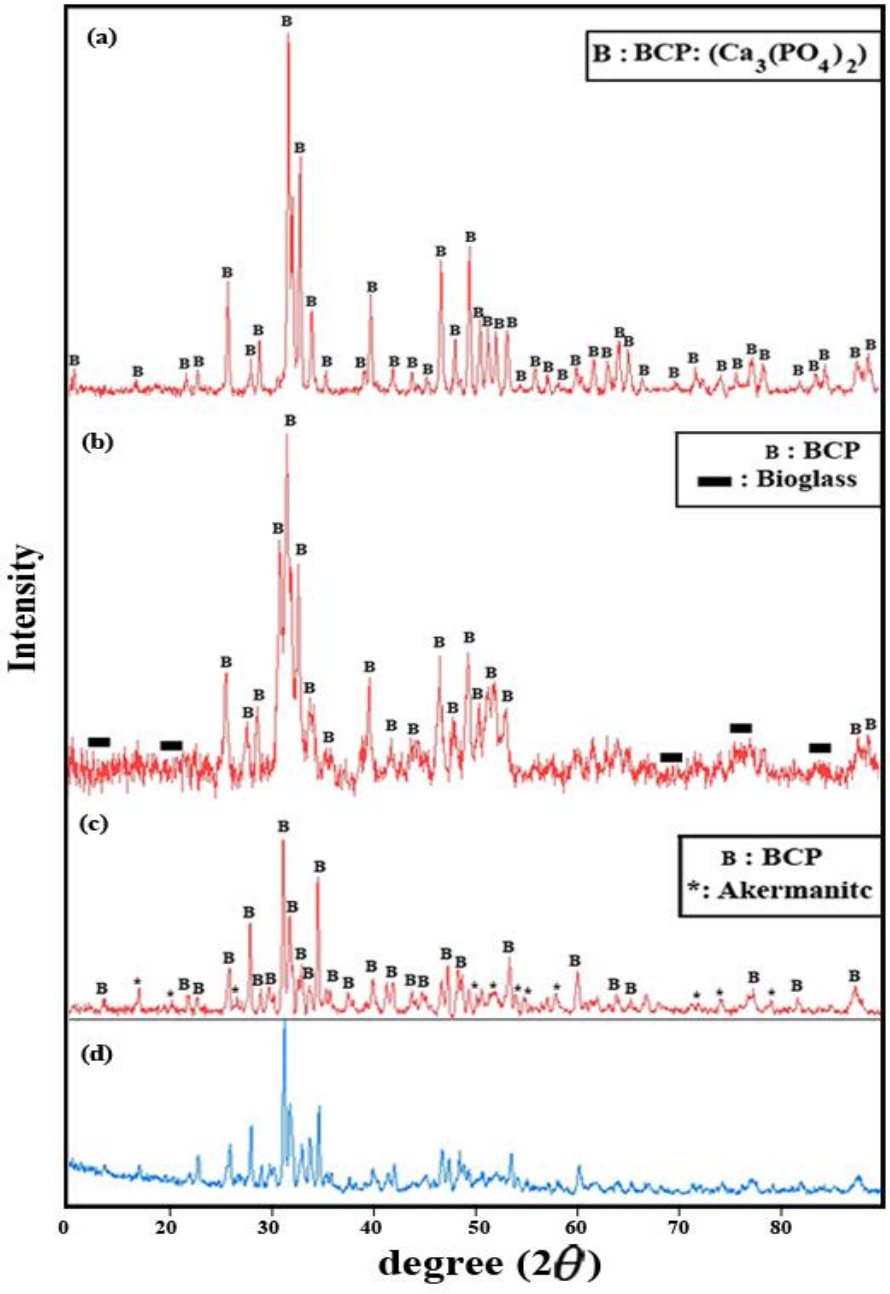

Fig. 5. XRD patterns: (a) scaffold B_0, (b) scaffold B_5, (c) scaffold B_5A_2 and (d) scaffold B_5A_5

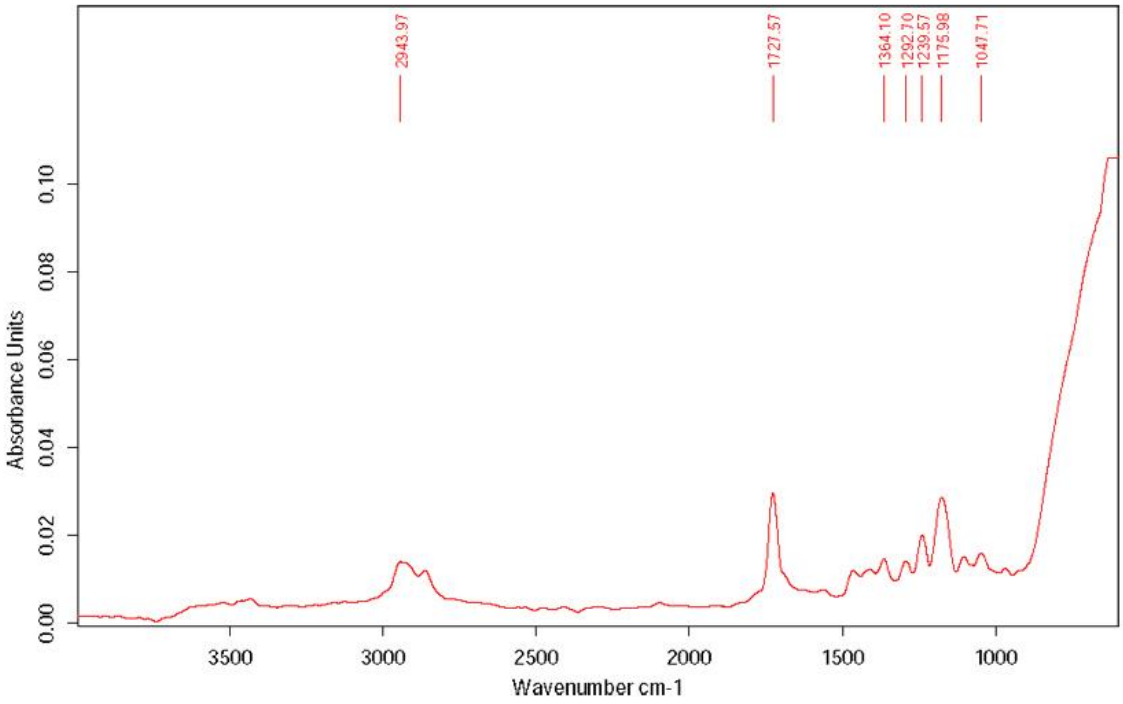

Fig. 6. ATR–FTIR spectrum of scaffold B_5A_2P

3.2. Characterization of scaffolds

Fig. 5(a) exhibits the XRD pattern related to scaffold B_0. In this pattern, it was observed that peaks had great match with BCP phase (JCPDS 00-025-0167). It can be explained that scaffold BCP was fabricated properly via polymeric sponge replication method. Comparison between Fig. 5(a) and Fig. 1(e) shows increasing peak height related to BCP phase. It can be argued that the fabrication of the scaffold via polymeric sponge method at high temperature (1200℃) causes more power of BCP phase formation, which is related to elements diffusion in BCP structure.

Fig. 5(b) indicates XRD pattern related to scaffold B_5. As observed in this figure, BCP phase (JCPDS 00-025-0167) was verified in the peaks. In scaffold B_5, 5wt% bioactive glass powder was used. It can be discussed that there were amorphous peaks among 60-90° angles more probably in the XRD pattern (Fig. 5(b)). In other words, amorphous peaks were in the background of the pattern. Utilizing 5wt% bioactive glass as reinforcing in scaffold BCP decreased peaks height due to being amorphous and not being crystalline.

Figs. 5(c) and 5(d) depict the XRD patterns related to scaffolds B_5A_2 and B_5A_5. In these patterns, BCP and akermanite phases were observed. In addition, it is possible that the amorphous peaks related to bioactive glass are in the background of the patterns. It can be concluded that composite scaffolds were fabricated via polymeric sponge replication method with success.

Fig.6 presents the ATR–FITR spectrum related to scaffold B_5A_2P. In the range of wavenumber of 1040 cm^{-1} to 1400 cm^{-1}, C – O – C symmetric stretching was found. Wavenumber of 1727 cm^{-1} was indicative of carbonyl group. In 2943 cm^{-1}, $-CH_2$ asymmetric stretching was observed [28, 29]. In ATR–FTIR spectrum, there were functional groups confirming the PCL coating in the fabricated scaffold.

Fig. 7(a) exhibits the SEM image relevant to the polymeric sponge. The sponge was spherical. On the other hand, the morphology of the sponge was indicant open with interconnected pores which can help the formation of scaffolds porous structure. Fig. 7(b) shows the SEM image related to scaffold B_0. Existing open pores and interconnectivity among them explain the porous structure of scaffold B_0. It seems that the scaffold structure is brittle because of high porosity and low compressive strength related to the scaffold. Fig. 7(c) illustrates the morphology of scaffold B_5. Similarly, there are open and interconnected pores in the scaffold structure. Fig. 7(d) demonstrates the SEM image related to scaffold B_5A_2. Formation of open pores with interconnectivity among them verifies the morphology of scaffold B_5A_2. It is worth noting that the mentioned scaffold possessed pores size range of 150–500 µm with respect to SEM images. This issue is useful and proper for bone tissue applications. The existence of open interconnected pores in the scaffolds structure

can help apatite deposit, cell migration and attachment, which can lead to new vascularization and repair of damaged bone tissues.

Fig. 7(e) exhibits the SEM image related to scaffold B_5A_5. As clearly observed in Fig. 7(e), many pores were clogged, and scaffold B_5A_5 structure is not porous. It can be argued that by enhancing akermanite content up to 5wt% to ceramic slurry, the slurry viscosity increased and resulted in clogging many pores.

Fig. 7(f) depicts the morphology of composite scaffold B_5A_2P. As observed in Fig. 7(f), there were open and interconnected pores with pore size range of 150–500 μm in the ceramic scaffold with PCL coating.

Despite the PCL coating on scaffold B_5A_2, it possesses a porous structure and can be affected by the formation of apatite in the scaffold pores and osteo-conduction.

High porosity is essential for scaffolds in bone tissue. In other words, the scaffolds should possess porous structures since connection among such structures, mechanical properties and bioactivity are significant. It can be stated that a scaffold should possess unique properties such as biocompatibility, bioactivity, high porosity and open and interconnected pores for bone tissue engineering applications so that apatite deposit, cell migration, proliferation and adhesion would be available to aim at new bone formation [30, 31].

Table 1. Porosity percentage of the scaffolds

Scaffold	Compressive Strength (MPa)
B_0	82.94
B_5	81.19
B_5A_2	80
B_5A_5	68.75
B_5A_2P	76.92

Table 2. Compressive strength values of the scaffolds

Scaffold	Compressive Strength (MPa)
B_0	0.12
B_5	0.31
B_5A_2	0.82
B_5A_5	0.97
B_5A_2P	1.9

Table 1 exhibits porosity percentage of the scaffolds. By increasing bioactive glass powder (5wt%) and akermanite powder (2wt%) to BCP slurry, porosity percentage decreased to a lesser extent (about 3wt%). Porosity is about 80% in scaffold B_5A_2. By enhancing bioceramics content to ceramic slurry, the slurry viscosity is increased so that porosity percentage is decreased to a large extent (about 15% for scaffold B_5A_5). Scaffold B_5A_2 was coated by PCL, and its porosity percentage was obtained about 76.92. By dip–coating the scaffold in PCL solution for 10 seconds, scaffold porosity has decreased (B_5A_2P) about 3% in comparison to scaffold B_5A_2. PCL has rarely-clogged pores related to scaffold B_5A_2.

Table 2 demonstrates compressive strength values of the scaffolds. As observed in this Table, scaffold BCP possessed low compressive strength about 0.12MPa. Hence, it can be concluded that its structure is brittle. By increasing the bioactive glass powder (5wt%) to ceramic slurry, the compressive strength of scaffold B_5 increased and was obtained about 0.3MPa. On the other hand, the strength is low and verifies the brittle structure related to scaffold B_5. By increasing akermanite powder to ceramic slurry, compressive strength improved from 0.3MPa to 0.8 and 0.97MPa for contents of 2wt% and 5wt% of akermanite, respectively. PCL coating performs an effective function in recovering the compressive strength of the ceramic scaffolds. It increased the compressive strength of scaffold B_5A_2 from about 0.8 to 1.9MPa. The strength was close to that related to spongy bone (2MPa) [32, 33]; hence, it can be applied in bone tissue engineering.

3.3. Bioactivity assessment

Scaffolds B_5A_2 and B_5A_2P were introduced as optimum scaffolds with respect to porosity percentage and compressive strength values in the present research, and bioactivity studies were carried out on them.

Fig. 8 presents the XRD pattern related to scaffold B_5A_2 soaked in SBF solution for 28 days. The peaks had great match with hydroxyapatite phase (JCPDS 01-076-0694). Those related to hydroxyapatite became strong after 28 days of soaking the scaffold in SBF, and the issue verified the formation of quasi–bone apatite on the surface of the scaffold. It can be concluded that scaffold B_5A_2 is a bioactive one for bone tissue engineering.

Fig. 9 exhibits SEM image related to soaked scaffold B_5A_2 in SBF solution for 28 days. The image clearly depicts an apatite–like layer on the surface of the scaffold.

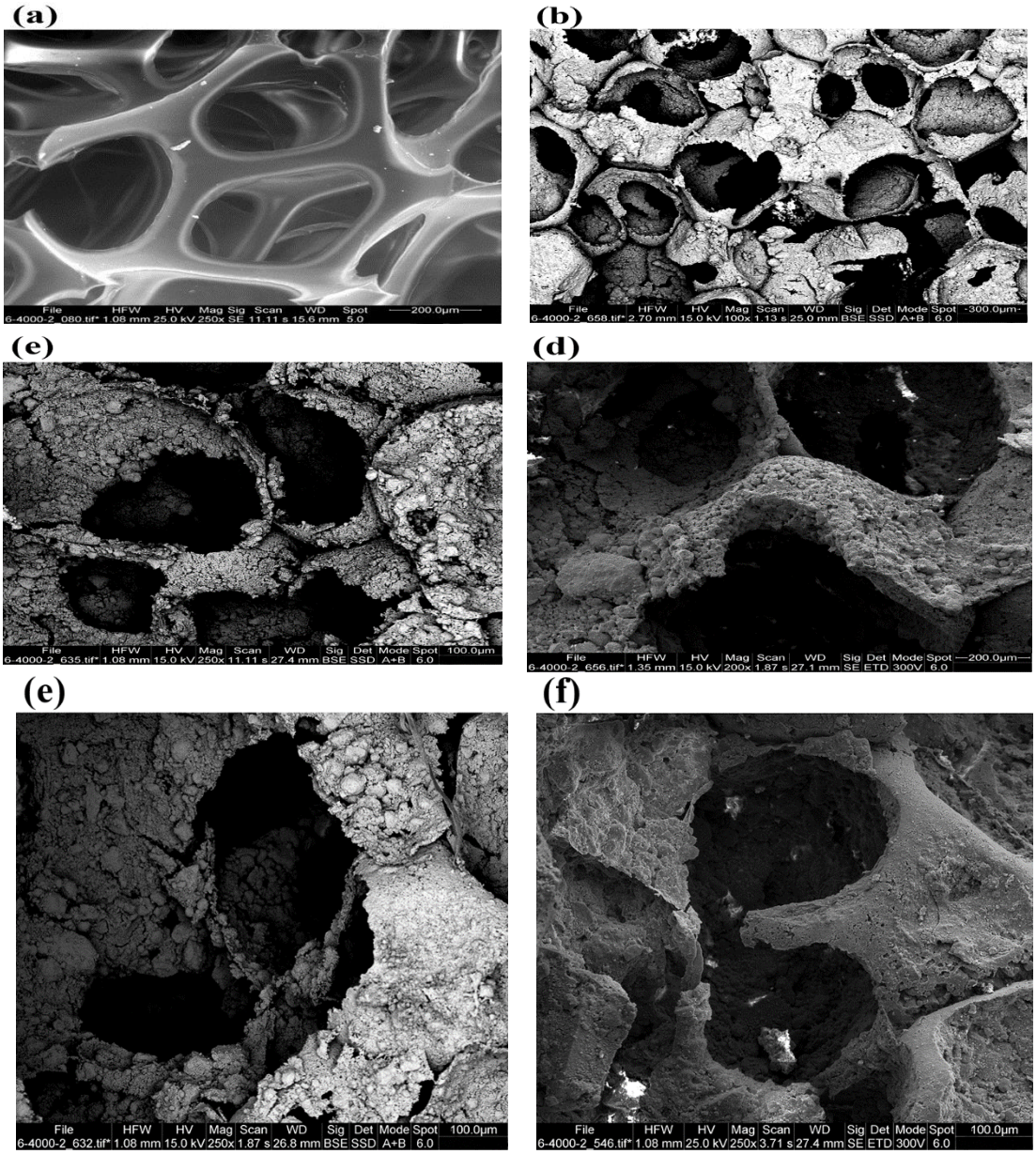

Fig. 7. SEM images: (a) polymeric sponge, (b) scaffold B_0, (c) scaffold B_5, (d) scaffold B_5A_2, (e) scaffold B_5A_5 and (f) scaffold B_5A_2P

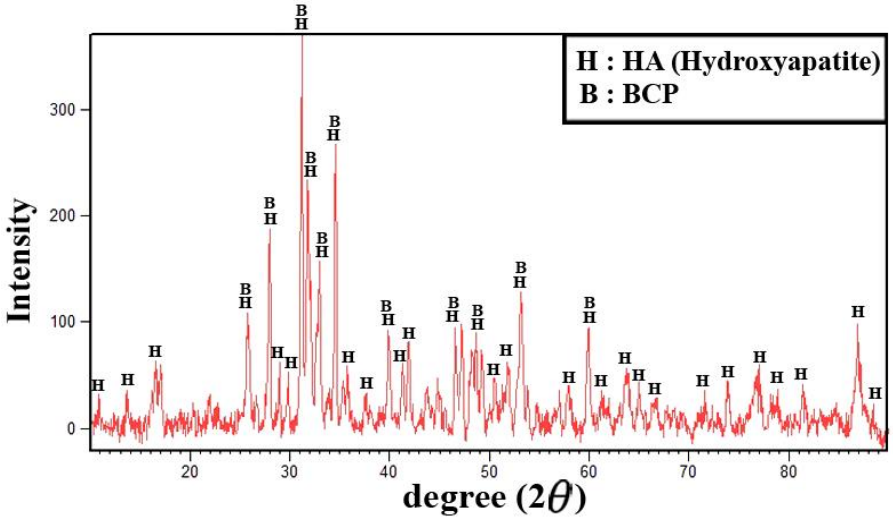

Fig. 8. XRD pattern of scaffold B_5A_2 soaked in SBF after 28 days

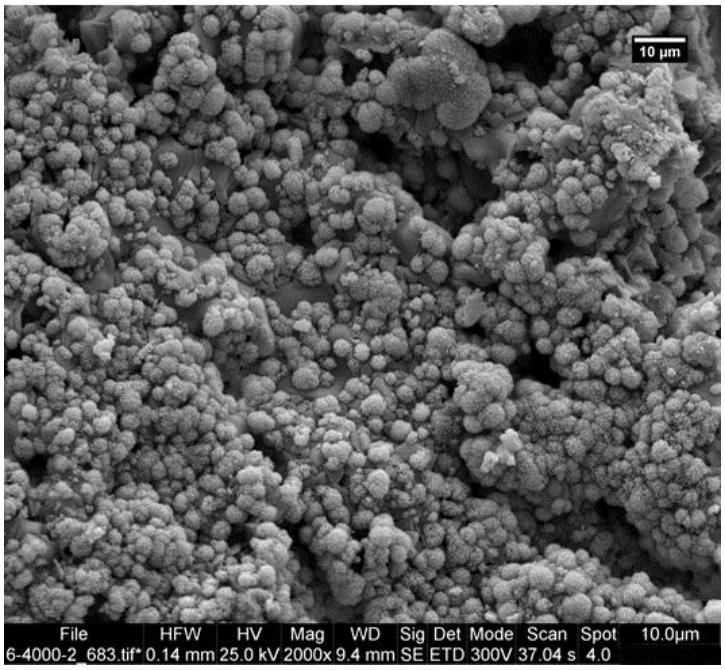

Fig. 9. SEM image related to scaffold B_5A_2 soaked in SBF after 28 days

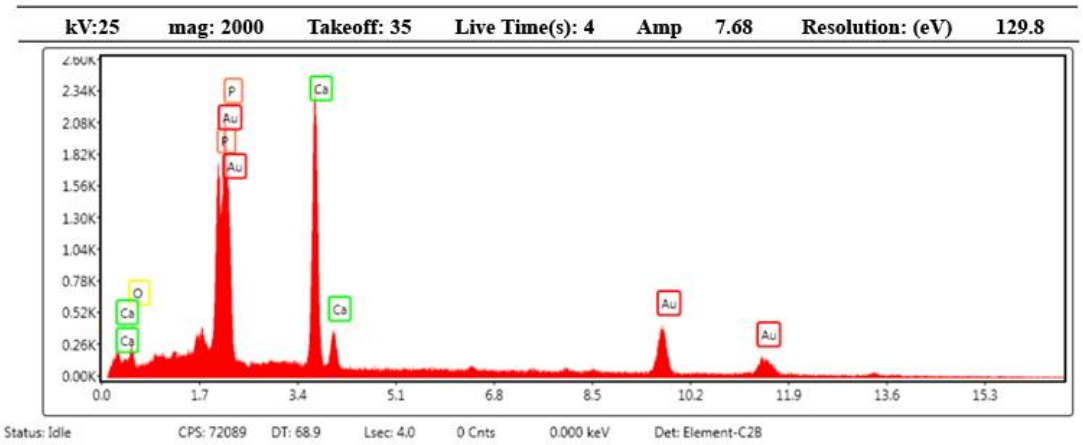

Fig. 10. EDS analysis of scaffold B_5A_2 soaked in SBF after 28 days

Table 3. Results of EDS analysis related to scaffold B_5A_2 soaked in SBF after 28 days

Element	Weight %	Atomic %	Net Int.
O K	6.39	22.38	254.45
P K	10.5	19	3472.12
CaK	31.41	43.91	6403.39
AuL	51.7	14.71	1740.27

Fig.10 and Table 3 show the results of EDS analysis related to scaffold B_5A_2 soaked in SBF for 28 days. It can be discussed that high atomic percent values related to calcium (Ca) and phosphorous (P) in EDS analysis proved the development of an apatite–like layer on the surface and in the pores of the scaffold (Ca/P = 2.31). The issue clearly confirms high bioactivity of porous scaffold B_5A_2.

Fig. 11 exhibits the XRD pattern related to scaffold B_5A_2P soaked in SBF solution for 28 days. The results of phase studies demonstrated high peaks related to hydroxyapatite phase (JCPDS 01-076-0694), which confirm quasi–bone apatite in the composite scaffold.

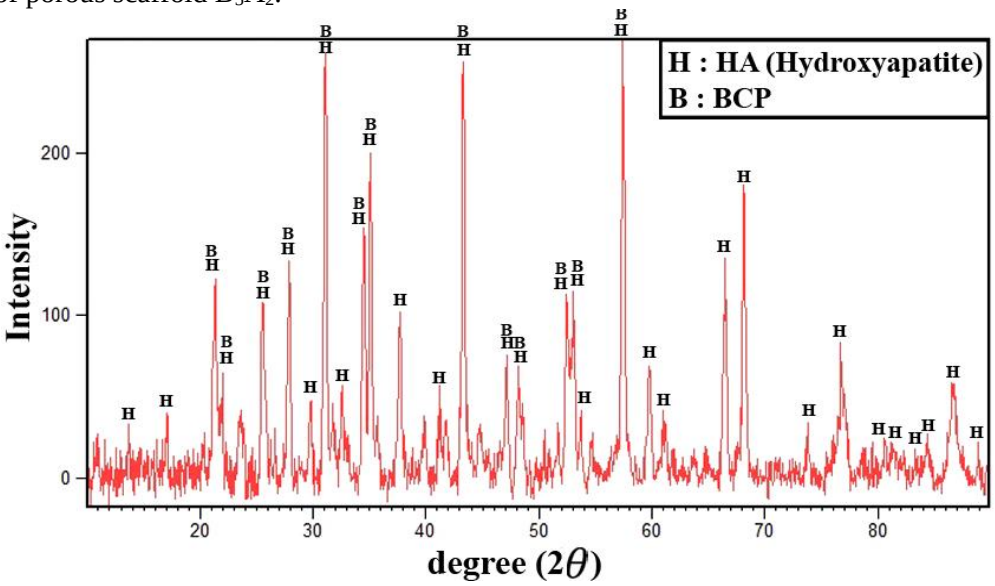

Fig. 11. XRD pattern relevant to scaffold B_5A_2P soaked in SBF after 28 days

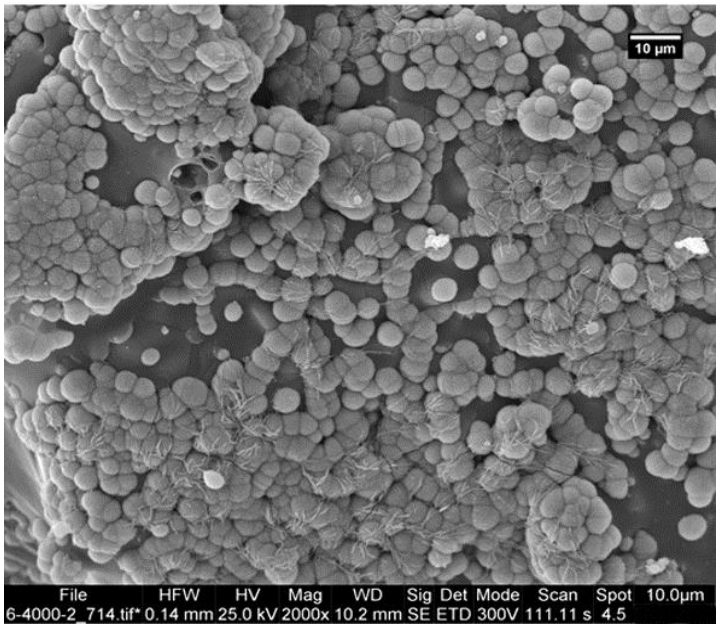

Fig. 12. SEM image of scaffold B_5A_2P soaked in SBF after 28 days

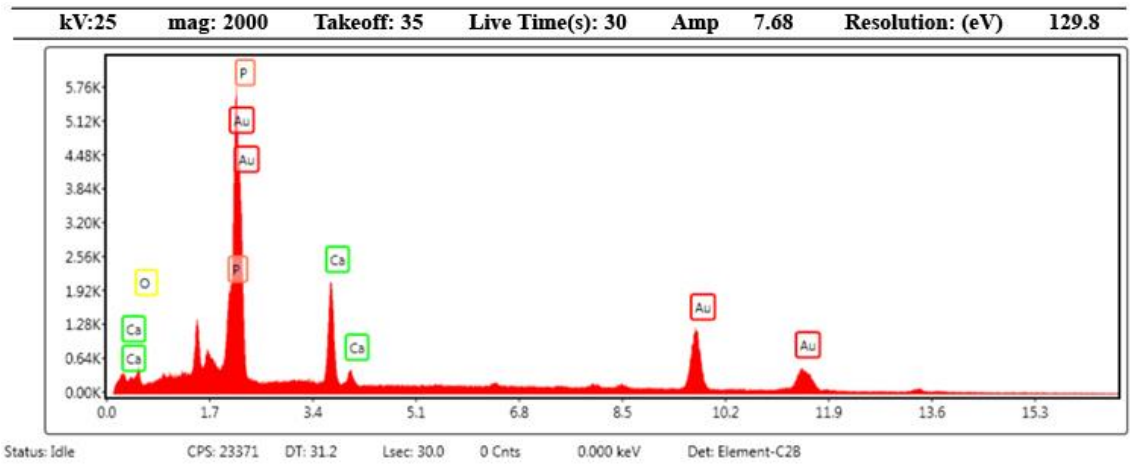

Fig. 13. EDS analysis related to scaffold B_5A_2P soaked in SBF after 28 days

Table 4. Results of EDS analysis relevant to scaffold B_5A_2P soaked in SBF after 28 days

Element	Weight %	Atomic %	Net Int.
O K	4.92	25.26	65.45
P K	4.8	12.74	408.64
CaK	14.91	30.56	722.53
AuL	75.37	31.44	709.04

Fig. 12 depicts the SEM image related to scaffold B_5A_2P soaked in SBF for 28 days. The image expresses that an apatite–like layer was developed on the surface of the composite scaffold.

Fig. 13 and Table 4 present the EDS analysis related to scaffold B_5A_2P soaked in SBF for 28 days. EDS results proved the development of an apatite–like layer on the surface and in the pores of the scaffold due to high atomic percent values related to Ca and P (Ca/P = 2.4), confirming the bioactivity of scaffold B_5A_2P for bone tissue engineering applications.

The mechanism of the formation of apatite expresses that silica group hydrolysis and the development of silanols (Si – OH) were carried out using the substitution of Ca^{2+} and Mg^{2+} instead of H^+ and H_3O^+ from SBF solution. A layer rich in silica is developed on the surface, and alkaline elements are vacated from the surface by a collection of Si – OH groups. Si – OH groups create the initial apatite crystals. In addition, releasing Ca^{2+} and Mg^{2+} was performed on Si – OH groups. Ca^{2+} and $(PO_4)^{3-}$ in SBF solution migrate to the surface through silica layer–rich and finally, a $CaO–P_2O_5$ film–rich is developed on the surface of silica layer–rich.

4. Conclusion

The present research focused on scaffolds such as biphasic calcium phosphate, bioactive glass–biphasic calcium phosphate, akermanite–bioactive glass–biphasic calcium phosphate and PCL–akermanite–bioactive glass–biphasic calcium phosphate with high porosity (80%), which were successfully fabricated and characterized by polymeric sponge replication and dip–coating methods.

Results showed that PCL coating enhanced the compressive strength of the ceramic scaffolds from 0.97 to 1.9MPa, verifying the fundamental role of PCL in improving the mechanical properties relevant to scaffolds in bone tissue engineering. The results of bioactivity evaluation confirmed the presence of apatite colonies on the surface of scaffolds, which proved the great bioactivity of the scaffolds. To conclude, akermanite (2wt%)–bioactive glass (5wt%)–biphasic calcium phosphate with PCL coating scaffold was introduced as the prime scaffold which can be applied for bone tissue engineering.

References

[1] E.M. Christenson, k.S. Aseth, J.J.P. Jeroen, V. D. Beucken, C.K. Chan, B. Ercan, J.A. Jansen, C.T. Laurencin, W.J. Li, R. Murugan, L.S. Nair, S. Ramakrishna, R.S. Tuan, T.J. Webster, A.G. Mikos, "Nanobiomaterials application in orthopedics", Journal of Orthopedic Research, Vol.25, pp.11-22, 2006.

[2] I. Seiler, J. Johnson, "Iliac crest autogenous bone grafting: donor site complications", Journal of South Orthopedic Association, Vol.9, pp.91-97, 2000.
[3] D. Hickey, B. Ercan, L. Sun, T. Webster, "Adding MgO nanoparticles to hydroxyapatite – PLLA nanocomposites for improved bone tissue engineering application", Journal of Acta Biomaterialia, Vol.14, pp.175 – 184, 2014.
[4] V. Guarino, F. Causa, I. Ambrosio, "Bioactive scaffolds for bone and ligament tissue", Journal of Expert Review of Medical Devices, Vol.4, pp.405-418, 2007.
[5] G. E. Rutkowski, C. A. Miller, S. K. Mallapragada, "Processing of polymer scaffolds: Solvent casting method of tissue engineering", San Diego, Academic Press, 2002.
[6] K. Whang, K. E. Healy, "Methods in tissue engineering processing of polymer scaffolds freeze – drying", San Diego, Academic Press, 2002.
[7] F. Schuth, K. S. W. Sing, J. Weitkamp, "Handbook of porous solids", Wiley – VCH, 2002.
[8] D. Bellucci, A. Sola, V. Cannillo, "A revised replication method for bioceramic scaffolds", Bioceramics Ashdin Publishing Bioceramics Development and Applications, Vol.1, 2011.
[9] I. Sopyan, M. Mel, S. Ramesh, K.A. Khalid, "Porous hydroxyapatite for artificial bone applications", Journal of Science Technology of Advanced Materials, Vol.8, pp.116 – 123, 2008.
[10] J.R. Jones, L.M. Ehrenfried, L.L. Hench, "Optimizing bioactive glass scaffolds for bone tissue engineering", Journal of Biomaterials, Vol.27, pp.964 – 973, 2006.
[11] R.K. Nalla, J.H. Kinnej, R.O., Ritchi, "Mechanistic fracture criteria for the failure of human cortical bone", Journal of Nature Materials, Vol.2, pp.164-168, 2003.
[12] M. Parvizifard, S. Karbasi, H. Salehi, S. Soleymani Eil Bakhtiari, Evaluation of physical, mechanical and biological properties of biogalss/titania scaffold coated with poly(3-hydroxybutyrate)-chitosan for bone tissue engineering, Mat. Tech: Adv.Perform.Mat., http://doi.org/10.1080/10667857.2019.1658169.
[13] S.A. Mali, K.C. Nune, R.D.K. Misra, Biomimetic nanostructured hydroxyapatite coatings on metallic implant materials, Mat. Tech: Adv. Perform. Mat. 31 (2016) 1-9.
[14] C. Bao, M. Chang, L. Qin, Y. Fan, E.Y. Teo, D. Sandikin, M. Choolani, J. K.Y. Chan, Effects of tricalcium phosphate in polycaprolactone scaffold for mesenchymal stem cell-based bone tissue engineering, Mat. Tech: Adv. Perform. Mat. 34 (2019) 361-367.
[15] S. Keikhaei, Z. Mohammadalizadeh, S. Karbasi, A. Salimi, Evaluation of the effects of Beta-tricalcium phosphate on physical, mechanical and biological properties of poly(3-hydroxybutyrate) / chitosan electrospun scaffold for cartilage tissue engineering applications, Mat. Tech: Adv. Perform. Mat. 34 (2019) 615-625.
[16] R. Iron, M. Mehdikhani, E. Naghszargar, S. Karbasi, D. Semnani, Effects of nano-bioactive glass on structural, mechanical and bioactivity properties of poly (3-hydroxybutyrate) electrospun for bone tissue engineering, Mat. Tech: Adv. Perform. Mat. 34 (2019) 540-548.
[17] Khajeh – Sharafabadi A, et.al. A novel and economical route for synthesizing akermanite ($Ca_2MgSi_2O_7$) nano – bioceramic. J Mater SCi Eng C. http:// dx.doi.org/10.1016/j. msec. 2016.11.021.
[18] Choudhary R, et.al. In vitro bioactivity, biocompatibility and dissolution studies of diopside prepared from biowaste by using sol-gel combustion method. J Mater Sci Eng C. 2016; 68: 89-100.
[19]A.K. Mohanty, M. Mirsa, G. Hinrichsen, "Biofibers, biodegradable polymers and biocomposites: an overview", Journal of Macromolecules Materials Engineering, Vol.276, pp.1-24, 2000.
[20] J.M. Anderson, M.S. Shive, "Biodegradation and biocompatibility of PLA and PLGA microspheres", Journal of. Advanced Drug Delivery Reviews, Vol.64, pp.72-82, 2012.
[21] T.K. Dash, V. Badireenath Konkimalla, "Polycaprolactone based formulations for drug delivery and tissue engineering: A review", Journal of Controlled Release, Vol.158, pp.15-33, 2012.
[22] L.C. Gerhardt, A.R. Boccaccini, "Bioactive glass and glass-ceramic scaffolds for bone tissue engineering", Journal of Materials Science, Vol.3, pp.3867-3910, 2010.
[23]A. Najafinezhad, M. Abdellahi, H. Ghayour, A. Soheily, A. Chami, A. Khandan, "A comparative study on the synthesis mechanism, bioactivity and mechanical properties of three silicate bioceramics", Journal of Materials Science Engineering C, Vol.72, pp.259 – 267, 2017.
[24] A. Sionkowska, J. Kozlowska, "Properties and modification of porous 3 – D collagen / hydroxyapatite composites", International Journal of Biological Macromolecules, Vol.52, pp.250 – 259, 2013.
[25] T. Kokubo, H.Takadama, "How useful is SBF in predicting in vivo bone bioactivity?", J. Biomaterials, Vol.27, 2907-2915, 2006.
[26] H. Ghomi, M. Jaberzadeh, M.H. Fathi, "Novel fabrication of forsterite scaffold with improved

mechanical properties", Journal of Alloys and Compounds, Vol.509, pp.63-68, 2011.
[27] M.H. Fathi, M. Kharaziha, "Two-step sintering of dense, nanostructural forsterite", Journal of Materials Letters, Vol.63, pp.1455-1458, 2009.
[28] Y.C. Lim, J. Johnson, Z. Fei, Y. Wu, D.F. Farson, J.J. Lannutti, H.W. Choi, L. Lee, "Micropatterning and Characterization of electrospun poly (epsilon – caprolactone)/ gelatin nanofiber tissue scaffolds by femtosecond laser ablation for tissue engineering applications", Journal of Biotechnology Bioengineering, Vol.108, pp.116126, 2011.
[29] L. Ghasemi – Mobarakeh, M.P. Prabhakaran, M. Morshed, M.H. Nasr – Esfahani, S. Ramakrishna, "Bio – functionalized PCL nanofibrous scaffold for nerve tissue engineering", Journal of Materials Science and Engineering C, Vol.30, pp.1129-1136, 2010.
[30] C. Vitale – Brovarone, M. Miola, C. Balagna, E. Verne, "3D – glass – ceramic scaffolds with antibacterial properties for bone grafting", Journal of Chemical Engineering, Vol.137, pp.129 – 136, 2008.
[31] C.V. Brovarone, E. Verne, P.F. Appendino, "Macro-porous bioactive glass – ceramic scaffolds for tissue engineering", Journal of Materials Science: Materials in Medicine, Vol.17, pp.1069 – 1078, 2006.
[32] D.R. Carter, W.C. Mayes, "Bone compressive strength: the influence of density and strain rate", Journal of Science, Vol.194, pp.1174-1176, 1976.
[33] L.L. Hench, J. Wilson, "An introduction to Bioceramics", world scientific, publishing, Co LTd, London, 1993.